THE ASTRONOMICAL JOURNAL VOLUME 110, NUMBER 6 DECEMBER 1995

CHEMISTRY AND KINEMATICS IN THE SOLAR NEIGHBORHOOD: IMPLICATIONS FOR STELLAR POPULATIONS AND FOR GALAXY EVOLUTION

ROSEMARY F. G. WYSE

Department of Physics and Astronomy,[1] The Johns Hopkins University, Baltimore, Maryland 21218; Institute of Astronomy, Madingley Road, Cambridge CB3 0HA, England, United Kingdom, and Center for Particle Astrophysics, University of California, Berkeley, California 94720

GERARD GILMORE

Institute of Astronomy, Madingley Road, Cambridge CB3 0HA, England, United Kingdom

Received 1995 March 13; revised 1995 August 7

ABSTRACT

The immediate Solar neighborhood should be a fair sample of the local Galaxy. However, the chemical abundance distribution of long-lived disk stars very near the Sun contains a factor of 5 to 10 more metal-poor stars, $-1 \lesssim [Fe/H] \lesssim -0.4$ dex, than is consistent with modern star-count models of larger scale Galactic structure. The metallicity distribution of complete samples of long-lived stars has long been recognized as providing unique constraints on the early stages of chemical evolution of the Galaxy, so that one would like to resolve this anomaly. We present a new derivation of the local G-dwarf metallicity distribution, based on the Third Gliese catalog combined with Olsen's (A&AS, 54, 55, 1983) Strömgren photometry. Kinematic data for these same stars, as well as for a high-precision sample studied by Edvardsson *et al.* (A&A, 275, 101, 1993), provide clear evidence that the abundance distribution below $[Fe/H] \sim -0.4$ contains two over-lapping distributions, the thick disk and the thin disk. However these samples in isolation do not allow a reliable deconvolution of the relative numbers in each population. We achieve this by comparing the local metallicity distribution with a recent determination (Gilmore, Wyse, & Jones, AJ, 109, 1095, 1995) of the metallicity distribution of stars, selected with the same evolutionary criteria as applied to our nearby star sample, but found *in situ* some 1500 pc from the Sun. The gravitational sieve of the Galactic potential acts on this second sample to segregate the low velocity dispersion, thin-disk, component of the local sample, leaving predominantly the second, higher velocity dispersion component. Thus the two samples are complementary, with the local sample providing accurate data primarily for the thin disk, but weak thin-disk/thick-disk discrimination, and the distant sample providing excellent thick-disk/thin-disk segregation. We are thus able to break the degeneracy between overlapping phase-space distributions. That is, the combination of these two datasets allows us to determine the source of the local paradox: there is a substantial tail of the thin disk (defined kinematically) metallicity distribution, which extends below $[Fe/H] \approx -0.4$ dex. This is a robust conclusion, being consistent with the sum of star count, stellar spatial density distribution, and both local and distant kinematic and chemical abundance data. Using the sum of this information, we deconvolve the local abundance distribution function into thin disk and thick disk components, and show these overlap considerably. This overlap has implications for some dynamical merger models of the formation of the thick disk. The observed scatter in the thin disk age–metallicity relation however obscures any simple interpretation in terms of thick disk formation models. The chemical abundance distributions derived in this paper, which are based on the sum of local and distant data, and so are directly integrated over the Solar Cylinder, improve long-standing constraints on Galactic disk evolution. When combined with age and element ratio data, comprehensive constraints on the evolution of the disk will be available.

1. INTRODUCTION

The metallicity distribution of complete samples of long-lived stars has long been recognized as providing unique constraints on the early stages of chemical evolution of the Galaxy. The main-sequence lifetime of F/G dwarf stars can be greater than the age of the Galaxy and hence such stars provide a complete record of the chemical evolutionary history (cf. van den Bergh 1962; Schmidt 1963; Pagel & Patchett 1975). Pioneering studies focused on the only reasonably complete sample available, which is that for stars in the immediate solar neighborhood; in effect stars within about 20 pc of the Sun. Until very recently, kinematic data were considered only as a means to quantify, and to correct for, biases in the sample used to derive the chemical abundance distributions. It is now appreciated however that the combination of chemical abundance and kinematic data is a substantially more powerful determinant of Galactic evolution than is either distribution considered in isolation. It is an improved determination of that bivariate distribution function, and its analysis, which is the theme of this paper.

The abundance data which have been available for the

[1]Permanent address.

 0004-6256/95/110(6)/2771/17/$0.90

complete sample of local stars, until now, have been derived from broadband photometric estimates, primarily using the 'ultraviolet excess' (Sandage 1969), derived in practice from somewhat heterogeneous *UBV* photometric data. The 'G-Dwarf Problem' was identified when these data were compared with the predictions of the Simple, Closed-Box model of chemical evolution, and has been characterized as 'the deficit of metal-poor stars in the solar neighborhood relative to the one-zone model of Galactic chemical evolution' (Pagel 1989).

The Simple, Closed-Box model has the virtue of analytic simplicity, and has the vice of being based upon physical assumptions that are inappropriate for a disk galaxy. It is somewhat of a 'straw man' model, easily knocked down, involving as it does several stringent assumptions. The assumptions inherent in this model are that:

(i) the system under study has zero metallicity initially;

(ii) the system is homogeneous at all times, i.e., there is no intrinsic scatter in the chemical enrichment of the interstellar medium, and specifically a unique correspondence between time and metallicity;

(iii) the system has a constant stellar Initial Mass Function (IMF);

(iv) the system has constant total mass at all times, i.e., flows of material do not occur;

(v) the Instantaneous Recycling Approximation is valid for nucleosynthesis products.

Lifting any (or all!) of these assumptions can provide for a very different metallicity distribution for long-lived stars. As we discuss further below, gas flows and spatial and temporal inhomogeneities in the interstellar medium are a natural feature of real disk galaxies. Even were the Simple Model predictions to fit some observational dataset, its inherent implausibility means that it is more likely that several compensating effects had generated this agreement by chance, rather than that the underlying physical processes corresponded to all the assumptions above. The important strength of the Simple Model lies in its ability to provide a convenient parametrization of the extent to which its assumptions fail, rather than in its ability to describe a dataset.

Chemical evolution models have been plagued with a myriad of assumptions and parameters, which leads to a lack of uniqueness (Tosi 1988). In order to improve one's understanding of Galactic evolution, one must consider the plausibility of the physics behind the model assumptions, and subject the model to a range of observational tests. Many of the simplest, single-parameter, adjustments to the Simple Model can be excluded by considering the totality of relevant data. For example, allowing the IMF to vary with time, as first discussed by Truran & Cameron (1971) in the context of prompt initial enrichment, is in conflict with the element ratio data which are now available for metallicities spanning -3 dex to above solar (Nissen *et al.* 1994). Similarly, one cannot posit 'pre-enrichment' as a solution to the G-dwarf problem without identifying a plausible source: stellar evolution in the stellar halo does not suffice (Hartwick 1976). It is clear, however, that detailed analysis of local chemical abundance data does provide important constraints on Galactic evolution, and is a worthwhile exercise.

The primary limitation of the nearby star sample utilized in studies of the local chemical abundance distribution is its small size. This inevitably means that stars which are either intrinsically rare—such as halo population subdwarfs—or stars which are common in the Galaxy as a whole, but whose spatial distribution and kinematics are such that their local volume density is small—such as thick disk stars—are poorly represented. Most recent and current efforts to extend present volume-limited samples to include minority populations have, for practical observational reasons, utilized kinematically defined samples of stars observed in the solar neighborhood. Subsequent correction for the kinematic biases inherent in these samples requires careful modelling (cf. Norris & Ryan 1991; Ryan & Norris 1993; Aguilar *et al.* 1995). An *in situ* sample, truly representative of the dominant stellar population far from the Sun, is required before one can be confident that these large, and model-dependent, corrections to local samples are reliable.

We have recently determined the (spectroscopic) iron abundance distribution for a sample of F/G stars *in situ* 1–5 kpc from the Galactic Plane (Gilmore *et al.* 1995). These data provide the volume-complete metallicity distribution at $z \gtrsim 1$ kpc which is complementary to local samples, and which allows a quantitative assessment of the reliability of corrections to solar neighborhood samples to account for their inherent kinematics biases, and of the statistical validity of the local sample. Combined with the local sample, these new data provide a powerful test of the integrated chemical evolution and star formation history of the local Milky Way.

As discussed below, recent determinations of the solar neighborhood abundance distribution have isolated (but not noted) an anomaly: while the derived distribution of chemical abundances for long-lived stars in a column through the Galactic disk at the Sun has reinforced the reality of the deficit of metal-poor stars, relative to Simple Model expectations, it has also derived a fraction of metal-poor stars which is a factor of nearly an order of magnitude too high for consistency with star-count models which explain data for distant stars. Typical star-count models derive a local ratio of thick disk to thin disk stars which is a few percent (e.g., reviews by Gilmore, *et al.* 1989; Gilmore 1990; Majewski 1993). Kinematic studies (Carney, *et al.* 1989; Freeman 1991; Edvardsson *et al.* 1993) suggest the thick disk becomes apparent at abundances below $[Fe/H] \approx -0.4$. As discussed below, recent analyses of local chemical evolution, in contrast, derive a fraction of typically 25 percent of 'disk' stars with $[Fe/H] \leqslant -0.4$ (Pagel 1989; Sommer-Larsen 1991). Thus, the local abundance distribution for disk stars apparently contains too many 'thick disk' stars to be consistent with other, well-established, analyses of Galactic structure. We quantify and resolve this discrepancy in this study.

The present paper builds upon previous work deciphering the chemical evolution of the Galactic disk. We provide a new determination of the solar-neighborhood metallicity distribution, derived from high-precision, intermediate-band photometry of long-lived stars (see also Wyse & Gilmore 1994). We compare this distribution with our data for distant F/G dwarfs, scaled down to the Galactic plane, and combine these two datasets. We use the joint distribution to derive the

abundance distribution of metal-poor thin disk stars, showing this is consistent with the distribution required by star count models. We then deduce the constraints on the formation of the thick disk, and the early evolution of the thin disk, which follow from this deconvolution.

2. THE SOLAR NEIGHBORHOOD G-DWARF METALLICITY DISTRIBUTION

2.1 Previous Determinations

Previous analyses have shown the power, and limitations, of local samples of F/G dwarfs in constraining the chemical evolution of the disk. The sample of Pagel & Patchett (1975) is the most often utilized. This consists of G stars drawn from various catalogs, the complete sample (to distances of 25 pc) being 133 stars from the RGO catalog of nearby stars, with metallicities derived from UV excess. The derived metallicity distribution of the 'solar cylinder'—that volume of unit circular cross section centered on the Sun's position and extended vertically through the extent of the disk—is taken from their Fig. 6 and shown here in Fig. 1(a). Note that only the binned data were published by Pagel and Patchett, and that those presented here are uncorrected for observational error and/or intrinsic scatter. The use of UV excess provides only rather inaccurate metallicity estimates (denoted $[Fe/H]_\delta$); Norris & Ryan (1989) derive a typical error of 0.45 dex for metallicities estimated with this technique, at least for their sample of interest, with $[Fe/H]_\delta < -0.4$ dex. Thus, the resulting abundance distribution will be substantially broadened, by measurement uncertainties, relative to the true underlying distribution. Since the width of the predicted distribution function is one of the characteristic differences between the simple model and more realistic models, such as those involving flows (e.g., Edmunds 1990) or inhomogeneities even in a closed system (e.g., Tinsley 1975), the precision of the abundance calibration is of major importance. Pagel and Patchett adopted a broadening of only 0.2 dex for the combination of measurement uncertainty and intrinsic scatter.

In an extension of his earlier work, Pagel (1989) adopted a recalibration of the relationship between [Fe/H] and UV excess due to Cameron (1985). From the same photometric data as his earlier work, he derived the metallicity distribution shown in Fig. 1(b). In addition to the considerable random uncertainties from the UV excess abundance calibration, Cameron's calibration is systematically $\lesssim 0.2$ dex more metal poor in [Fe/H], for given UV excess, than the more widely used calibration of Carney (1979). Despite the large scatter referred to above, Norris & Ryan (1989) found no *systematic* offset between $[Fe/H]_\delta$ based on the Carney calibration and their spectroscopically determined metallicities. Again, their sample was limited to stars with $[Fe/H]_\delta < -0.4$ dex, but it is just these stars which are of greatest interest for the solar cylinder G-dwarf metallicity distribution.

The metallicity distributions reproduced in Figs. 1(a) and 1(b) are not in fact those obtained directly from the photometric data for the local sample, but are for the 'solar cylinder' and have been weighted (by Pagel) to attempt to take account of the kinematic bias introduced by the solar neighborhood selection—high velocity stars, which spend only a small fraction of their orbit in the vicinity of the Sun will be under-represented. In the simplest picture of disk structure and evolution there are no radial flows, or gradients in either density or kinematics, and an integrated history of the disk is obtained by study of the stars in unit area of the plane, rather than unit volume. If density profile data were available, then one could simply integrate. However, such data were not available until the mid 1980s, so Pagel (following Schmidt 1963) weighted the input binned metallicities by the mean

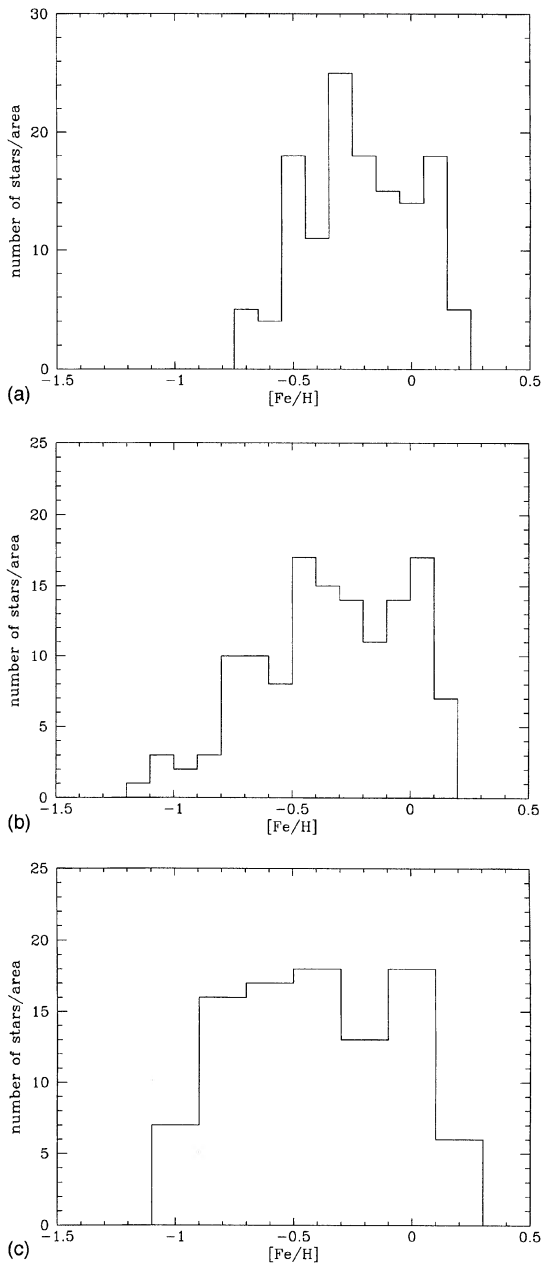

FIG. 1. (a) The solar cylinder metallicity distribution from Pagel & Patchett (1975). (b) The same data as (a), but with a different metallicity calibration, from Pagel (1989). (c) The same data and metallicity calibration as (b), but with a different kinematic weighting, from Sommer-Larsen (1991).

vertical velocity of stars in that bin. However, this correction is only appropriate for motion in a harmonic potential (constant period for all orbits), which corresponds to a constant density distribution of gravitating material. While this may be a reasonable approximation for low-velocity stars that do not penetrate much beyond a disk scale height, it is a rather poor approximation for just those high-velocity stars for which the weighting is most important. In particular, the thick disk and halo remain under-represented (cf. Gilmore & Wyse 1986; Gilmore 1990).

Sommer-Larsen (1991; see also Sommer-Larsen & Antonuccio-Delugo 1993) followed Pagel's (1989) sample selection and UV-excess calibration, and so analyzed the same basic metallicity distribution. Again, they followed Pagel (1989) in recognizing that the photometrically determined metallicity correlated most strongly with the *iron* abundance, which is perhaps the element least likely to be well-described by the Instantaneous Recycling Approximation, inherent in the chemical evolution models that are most often compared with the metallicity distributions, given that Type Ia supernovae are an important site for iron synthesis. Rather than calculating predictions from more realistic chemical evolution models, Sommer-Larsen instead adopted a mean relationship between oxygen, produced predominately in massive stars by Type II supernovae, and iron, and transformed the photometric metallicity/iron distributions into 'oxygen' distributions (cf. Pagel 1989). It is now clear from the Edvardsson *et al.* (1993) data that the relationship between oxygen and iron varies as a function of radius in the Galaxy, as expected if the star formation rate in the galactic disk varies as a function of radius, being higher in the central regions (cf. Wyse 1995). The adoption of a single-valued relationship introduces uncertainties of perhaps 0.2 dex for the more metal-poor stars in the sample. We here have reverse-transformed the oxygen abundance distributions of Sommer-Larsen (1991) back to photometric-metallicity distributions. Sommer-Larsen (1991) improved upon the harmonic potential weighting by calculating the potential of a self-gravitating disk that had the observed stellar-density profile of Kuijken & Gilmore (1989). This provides more weight to the 'hotter' metal-poor stars, and results in the metallicity distribution shown in Fig. 1(c).

We return to discussion of the appropriate distribution of chemical abundances to describe the Solar neighborhood below. However, we note here that the fractions of stars more metal poor than -0.4 dex, where thick disk kinematics are apparent (see below), in these weighted distributions are approximately 25% (Pagel and Patchett), 40% (Pagel), and 50% (Sommer-Larsen). Were this to be taken as an estimate of the relative mass of the thick disk to that of the thin disk, one would conclude that the thick disk is of order the same mass as the thin disk. As we discuss below, this would be somewhat difficult to understand in the light of star count analyses and *in situ* studies of the thick disk.

2.2 A New Determination—Sample Selection

Photometric catalogs of nearby stars have progressed substantially in both precision and reliability in the almost 20 years since Pagel and Patchett obtained their chemical abundance distribution function. Intermediate-band Strömgren photometry provides a more accurate estimation of the metallicity of a F/G star than does the broadband color-based UV excess, and is now available for many nearby stars. The sample of long-lived, main-sequence stars in the immediate solar neighborhood, for which carefully checked data are given in the current version of the Gliese catalog, has been extended from the distance limit of about 20 pc, available at the time of the Pagel and Patchett study, to distances of about 30 pc. As such, the Gliese catalog provides the ideal local sample, superseding the RGO catalog. Hence we combined the most reliable census of nearby stars with the most precise photometric data, by cross-correlating the Third Gliese catalog (Nearby Stars 3, obtained from NSSDCA) with the *uvby*(β) photometry catalog of Olsen (1983; also obtained from NSSDCA). Both catalogs were searched to identify all single, normal stars (no white dwarfs) with $V \leqslant 9$; $0.4 \leqslant B-V < 0.9$, which appeared in both.

This produced 128 stars; one which is known to have an erroneous parallax tabulated was immediately deleted (HD 140283; see Gilmore *et al.* 1991), leaving a sample of 127 F/G dwarfs. For comparison, the sample of Pagel and Patchett, and later authors, contained 133 stars with data from heterogeneous sources.

2.3 Metallicity Estimator

The most precise and reliable metallicity indicator which is available for essentially the whole sample of nearby stars is the relationship between [Fe/H] and Strömgren photometric index $(b-y)$. We have adopted the calibration of this photometric metallicity estimator due to Schuster and Nissen (1989a). This estimator, [Me/H], is given by the following expression for stars with $0.22 \leqslant (b-y) \leqslant 0.375$:

$$\begin{aligned}[\mathrm{Me/H}] = {} & 1.052 - 73.21 m_1 + 280.9 m_1 (b-y) \\ & + 333.95 m_1^2 (b-y) - 595.5 m_1 (b-y)^2 \\ & + [5.486 - 41.62 m_1 - 7.963 (b-y)] \log(m_1 \\ & - c_3),\end{aligned}$$

where $c_3 = 0.6322 - 3.58(b-y) + 5.20(b-y)^2$, and by the following when $0.375 < (b-y) \leqslant 0.59$:

$$\begin{aligned}[\mathrm{Me/H}] = {} & -2.0965 + 22.45 m_1 - 53.8 m_1^2 \\ & - 62.04 m_1 (b-y) + 145.5 m_1^2 (b-y) \\ & + [85.1 m_1 - 13.8 c_1 - 137.2 m_1^2] c_1 .\end{aligned}$$

Note that this calibration does not require a measurement of β, the Strömgren index that is most sensitive to effective temperature. The β index, being narrowband rather than intermediate band, is available for fewer stars than are *uvby* data.

Edvardsson *et al.* (1993) provide a metallicity calibration for F/G stars that does utilize β, and it is possible to make a direct comparison between the two techniques. The Edvardsson *et al.* estimator is

$$[\mathrm{Me/H}] = -[10.5 + 50(\beta - 2.626)] \times \delta m_1 + 0.12,$$

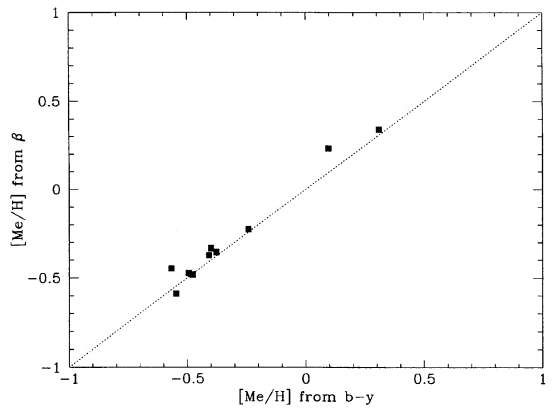

FIG. 2. Metallicity estimated using the technique of Edvardsson *et al.* against that obtained using the technique of Schuster and Nissen.

where $\delta m_1 = m_{1,\mathrm{Hyades}}(\beta) - m_1$, with the Hyades sequence taken from Crawford & Barnes (1969); note that their relationship between m_1 and β for the Hyades is well-behaved for $2.6 \leq \beta \leq 2.89$ only.

The metallicity estimates obtained using these two techniques, for the ten stars in the present sample with β in the well-behaved Hyades range, and with $(b-y)$ within the Hyades range of 0.076–0.39 (Crawford & Barnes 1969) are shown in Fig. 2. The scatter about the dotted line which indicates perfect correspondence is less than 0.1 dex. Indeed, the mean difference between the two techniques for this subsample is 0.04 dex, with a dispersion of 0.05 dex. Thus adopting the Schuster and Nissen metallicity calibration is justified.

Further, Edvardsson *et al.* investigated the calibration of their photometric metallicity estimate by comparison with their spectroscopic iron abundance estimates. They found, after removal of 15 of their most metal-rich stars (all with metallicity above the solar value), very good agreement:

$$[\mathrm{Me/H}] = 1.049[\mathrm{Fe/H}] - 0.030; \quad \sigma = 0.074 \quad n = 174.$$

This result is valid for their entire range of iron abundances, including the bulk of their metal-rich stars. Without removal of those 15 metal-rich stars, for which the photometric indices yield an overestimate of the iron abundance by 0.1–0.3 dex, it can be seen from their Fig. 6 that the scatter increases to ~0.15 dex above solar metallicity, with a mean offset of ~0.05 dex.

There are four stars in the present sample that have spectroscopic iron abundances available from Edvardsson *et al.* These are HD 6434, with a spectroscopic [Fe/H] = −0.54 dex, HD 22879, with a spectroscopic [Fe/H] = −0.84 dex, HD 89707, with a spectroscopic [Fe/H] = −0.42 dex and HD 165401, with a spectroscopic [Fe/H] = −0.47 dex. Comparison of our metallicity estimates with the iron abundances yields a mean offset of 0.003 dex (their estimate being the one slightly more metal poor) and a dispersion of only 0.04 dex. Thus the metallicity estimate adopted here based on intermediate-band photometry is a reliable and precise ($\sigma \lesssim 0.1$ dex) indicator of *true iron abundance*.

Applying the Schuster and Nissen calibration to the F/G star sample extracted from the Gliese catalog provides the metallicity estimates given in Table 1, which also contains the necessary photometric data for the stars. The addition of the Sun brings the sample to 128 stars and results in the metallicity distribution shown as a histogram in Fig. 3.

2.4 *Isolation of Potentially Long-Lived Stars*

In order for the metallicity distribution function to be an unbiased description of the chemical history, the sample must be restricted to include only those stars which have both masses and metallicities such that any star ever formed, which has those parameters, is still on the main sequence today. If this restriction were not applied, then some parts of age–metallicity space would be excluded from measurement, potentially distorting the resulting metallicity distribution function. It should be emphasized that the selection of a restricted range of spectral types does *not* achieve this, due to metallicity-dependent evolutionary times. Spectral types in the absence of metallicity data are not a sufficiently good indicator of mass, or of main-sequence lifetimes.

An estimate of the age of the disk, based on (VandenBerg) stellar evolution models, is available from the data of Edvardsson *et al.* (1993). This sample of 189 stars was drawn from the Olsen local sample and was designed to cover the metallicity range above one-tenth of solar uniformly; thus there should be no kinematic-metallicity bias. As discussed in some detail by Freeman (1991), the kinematic thin disk/thick disk transition in that sample occurs fairly abruptly at 12 Gyr, which may be taken as a minimum age for the thin disk.[2] Thus the evolutionary selection was effected by removing stars which had a potential main-sequence lifetime less than 12 Gyr, according to the VandenBerg & Bell (1985) isochrones ($Y = 0.20$), the VandenBerg (1985) isochrones ($Y = 0.25$) and the VandenBerg & Laskarides (1987) isochrones. Colors for models of solar metallicity and above were initially obtained by interpolation in Table 1 of VandenBerg & Bell (1985), using the effective temperature and gravity of turnoff stars from VandenBerg (1985; solar metallicity) and from VandenBerg & Laskarides (1987; three times solar metallicity). Interpolation in this table predicts a solar color of $(b-y)_\odot = 0.388$, to be compared with a measured color of $(b-y)_\odot \simeq 0.405 \pm 0.002$ (Saxner & Hammarbäck 1985; Magain 1987). We took this difference in solar color as a zero-point color offset, and thus adjusted the interpolated $(b-y)$ colors by adding 0.017 (cf. Schuster & Nissen 1989b). Note that there is no agreement in the zero point of the theoretical models in c_1 with the present data. Fortunately for our purposes we need to use only the $(b-y)$ color information, as only the turnoff temperature is required and we have metallicity data. The adjusted turnoff $(b-y)$ colors obtained this way are given in Table 2, for convenience. These models show an increasing, and probably overestimated, sensitivity of $(b-y)$ to metallicity, with increasing metallicity. In par-

[2]Note that the Edvardsson *et al.* data show no evidence for an age gap between the thick disk and the thin disk, either in the direct age estimates, or in the element ratios (see Wyse, 1995, for further discussion of this point). The data of Marquez & Schuster (1994) also show considerable overlap in age between the halo and thick disk, with a continuous age distribution, into the thin disk.

TABLE 1. Gliese catalog F/G dwarfs.

HD	B−V	$(b-y)$	m_1	c_1	β	[Me/H]	rejected?	W vel	HD	B−V	$(b-y)$	m_1	c_1	β	[Me/H]	rejected?	W vel
1273	0.64	0.409	0.182	0.248	2.592	−0.57	no	−5	64606	0.73	0.450	0.221	0.217	...	−0.76	no	−5
1388	0.59	0.379	0.191	0.345	...	−0.01	yes	...	65583	0.71	0.449	0.234	0.229	2.548	−0.61	no	−35
3079	0.54	0.364	0.156	0.367	2.607	−0.41	no	12	66751	0.58	0.372	0.151	0.265	2.585	−0.52	no	9
3823	0.56	0.359	0.156	0.348	2.609	−0.38	yes	...	67458	0.60	0.375	0.189	0.302	...	−0.07	yes	...
4208	0.67	0.404	0.227	0.278	...	−0.10	no	...	68456	0.43	0.290	0.143	0.453	...	−0.31	yes	...
6434	0.60	0.383	0.159	0.275	2.586	−0.53	no	−10	69830	0.76	0.458	0.297	0.307	...	0.01	no	...
10800	0.61	0.390	0.201	0.302	...	−0.10	yes	...	73524	0.60	0.376	0.202	0.376	...	0.17	yes	...
11112	0.65	0.409	0.200	0.400	...	−0.05	no	...	77137	0.69	0.438	0.234	0.362	...	0.02	no	...
13043	0.61	0.388	0.206	0.379	...	0.14	yes		78612	0.61	0.384	0.185	0.313	...	−0.17	yes	...
13445	0.82	0.486	0.338	0.283	...	−0.17	no	...	88261	0.60	0.376	0.168	0.295	...	−0.34	no	...
14412	0.73	0.445	0.247	0.231	...	−0.52	no	−10	88697	0.49	0.326	0.163	0.437	...	−0.12	yes	...
14802	0.60	0.390	0.185	0.379	...	−0.11	yes	...	88725	0.60	0.394	0.166	0.256	2.577	−0.59	no	−24
16141	0.67	0.424	0.211	0.377	2.594	−0.05	no	...	88742	0.59	0.379	0.181	0.334	...	−0.14	yes	...
16397	0.60	0.388	0.156	0.281	2.578	−0.58	no	−31	89707	0.55	0.360	0.148	0.307	2.603	−0.48	no	54
16417	0.65	0.413	0.205	0.397	...	−0.02	no	...	94444	0.52	0.343	0.135	0.316	2.605	−0.55	no	−8
16784	0.56	0.380	0.131	0.302	2.597	−0.82	no	22	94518	0.60	0.378	0.179	0.288	...	−0.26	no	...
17051	0.56	0.356	0.190	0.363	2.637	0.10	yes		96700	0.60	0.389	0.176	0.319	...	−0.29	no	...
17865	0.55	0.371	0.141	0.309	2.593	−0.61	no	−23	97343	0.77	0.458	0.300	0.313	...	0.04	no	
17925	0.87	0.511	0.390	0.297	...	−0.14	no	...	100004	0.41	0.279	0.126	0.466	2.674	−0.57	yes	−2
18803	0.72	0.429	0.267	0.326	...	0.16	no	...	102438	0.68	0.426	0.220	0.273	...	−0.31	no	...
19467	0.65	0.409	0.200	0.337	...	−0.13	no	...	104304	0.77	0.464	0.312	0.345	2.583	0.17	no	...
20165	0.86	0.508	0.407	0.297	...	−0.14	no	...	110010	0.59	0.395	0.228	0.387	2.609	0.31	yes	...
20407	0.58	0.373	0.162	0.280	2.605	−0.40	no	−11	112164	0.64	0.392	0.209	0.458	...	0.16	yes	...
20619	0.66	0.405	0.215	0.276	...	−0.19	no	...	114174	0.67	0.418	0.233	0.335	2.589	0.07	no	...
20794	0.71	0.440	0.235	0.283	2.575	−0.26	no	...	116459	0.50	0.339	0.165	0.399	...	−0.15	yes	...
22049	0.88	0.514	0.410	0.273	...	−0.24	no	...	117635	0.78	0.474	0.293	0.240	...	−0.47	no	−19
22484	0.57	0.370	0.169	0.379	...	−0.30	yes	...	117939	0.67	0.409	0.208	0.310	...	−0.14	no	...
22879	0.54	0.369	0.120	0.273	2.580	−0.81	no	−49	120690	0.69	0.434	0.236	0.301	...	−0.14	no	...
24293	0.66	0.412	0.211	0.332	...	−0.07	no	...	122742	0.74	0.451	0.272	0.319	...	0.02	no	...
30495	0.63	0.399	0.213	0.320	2.593	0.00	yes	...	122862	0.58	0.366	0.185	0.359	...	−0.05	yes	...
36435	0.77	0.454	0.300	0.263	...	−0.20	no	...	124292	0.74	0.446	0.269	0.295	...	−0.08	no	...
36767	0.54	0.344	0.168	0.336	...	−0.14	yes	...	129333	0.61	0.408	0.202	0.301	...	−0.21	no	...
37655	0.60	0.380	0.176	0.373	2.593	−0.17	yes	...	130948	0.56	0.376	0.192	0.324	...	−0.03	yes	...
42618	0.63	0.402	0.219	0.303	2.581	−0.03	yes	...	131511	0.84	0.499	0.371	0.294	...	−0.13	no	...
42807	0.67	0.414	0.228	0.293	2.582	−0.09	no	...	133002	0.68	0.442	0.192	0.345	2.567	−0.41	no	−18
43834	0.72	0.442	0.263	0.339	2.601	0.11	no	...	134483	0.50	0.322	0.165	0.395	...	−0.07	yes	...
46588	0.50	0.345	0.158	0.346	...	−0.27	yes	...	136352	0.65	0.403	0.195	0.294	2.592	−0.26	no	...
50806	0.72	0.432	0.235	0.368	...	0.08	no	...	143291	0.77	0.466	0.284	0.252	...	−0.38	no	...
52449	0.53	0.332	0.177	0.391	...	0.06	yes	...	144287	0.77	0.467	0.287	0.316	...	−0.03	no	...
52711	0.60	0.386	0.182	0.330	2.590	−0.18	no	...	145417	0.83	0.511	0.276	0.168	...	−1.28	no	...
56274	0.61	0.373	0.181	0.246	2.575	−0.17	yes	...	145675	0.88	0.528	0.393	0.409	2.575	0.11	no	...
61994	0.66	0.445	0.247	0.298	...	−0.16	no	...	145809	0.61	0.396	0.187	0.328	...	−0.20	no	...
62613	0.73	0.450	0.261	0.293	2.567	−0.14	no	...	146775	0.61	0.379	0.211	0.318	...	0.11	yes	...
62644	0.77	0.493	0.226	0.382	...	−0.36	no	...	150706	0.62	0.389	0.188	0.312	...	−0.18	no	...

TABLE 1. (continued)

HD	B−V	$(b-y)$	m_1	c_1	β	[Me/H]	rejected?	W vel
152391	0.76	0.457	0.294	0.290	...	−0.08	no	...
153597	0.48	0.327	0.154	0.364	2.627	−0.24	yes	...
153631	0.58	0.386	0.189	0.339	...	−0.09	yes	...
154345	0.73	0.448	0.273	0.286	2.565	−0.12	no	...
154577	0.89	0.519	0.389	0.227	...	−0.51	no	17
155918	0.60	0.385	0.153	0.269	2.590	−0.62	no	70
158633	0.76	0.460	0.286	0.244	2.550	−0.39	no	...
159222	0.65	0.404	0.219	0.364	2.595	0.13	yes	...
161612	0.71	0.439	0.259	0.359	...	0.17	no	...
162521	0.45	0.292	0.160	0.419	...	−0.06	yes	...
165401	0.62	0.391	0.170	0.286	2.581	−0.44	no	−38
166620	0.87	0.516	0.407	0.294	2.540	−0.16	no	...
167954	0.54	0.335	0.180	0.412	...	0.08	yes	...
171665	0.69	0.420	0.230	0.309	...	−0.05	no	...
172051	0.68	0.415	0.225	0.267	2.569	−0.23	no	...
176377	0.58	0.385	0.179	0.292	2.588	−0.30	no	...
177565	0.71	0.431	0.256	0.326	2.584	0.09	no	...
182488	0.81	0.481	0.348	0.331	2.567	0.08	no	...
189567	0.65	0.399	0.199	0.298	...	−0.19	no	...
190248	0.76	0.472	0.278	0.398	2.603	0.16	no	...
192310	0.88	0.521	0.428	0.295	...	−0.16	no	...
193307	0.55	0.363	0.148	0.349	2.604	−0.49	no	21
193664	0.58	0.386	0.184	0.315	2.593	−0.19	no	...
194640	0.73	0.440	0.274	0.301	...	0.01	no	...
195987	0.79	0.481	0.299	0.270	...	−0.31	no	...
196761	0.72	0.441	0.259	0.258	...	−0.28	no	...
197214	0.67	0.423	0.217	0.250	...	−0.42	no	11
199288	0.58	0.384	0.148	0.265	2.575	−0.68	no	43
199620	0.84	0.527	0.294	0.391	...	−0.10	no	...
202457	0.68	0.433	0.220	0.370	...	−0.04	no	...
205905	0.62	0.388	0.219	0.329	...	0.15	yes	...
210277	0.75	0.472	0.275	0.382	...	0.11	no	...
210918	0.65	0.398	0.221	0.320	...	0.07	yes	...
213628	0.72	0.441	0.266	0.315	...	0.03	no	...
213941	0.66	0.418	0.193	0.270	...	−0.46	no	−69
218209	0.65	0.419	0.189	0.258	2.568	−0.54	no	−14
220339	0.89	0.515	0.414	0.251	...	−0.34	no	...
221613	0.58	0.394	0.183	0.286	...	−0.33	no	...
223731	0.43	0.293	0.138	0.428	...	−0.38	yes	...

ticular, the large increase in $(b-y)$ based on the VandenBerg and Laskarides models of above solar metallicity does not agree with the trend predicted by the observationally calibrated model atmospheres of Edvardsson *et al.* (1993). This latter study finds $\Delta(b-y)/\Delta[\mathrm{Me/H}]=+0.026$ mag/dex, for stars with iron abundance in the range from solar metallicity to +0.17 dex. It should be noted that since the VandenBerg (1985) isochrones have a $1.\mathcal{M}_{\odot}$ star of solar metallicity at the

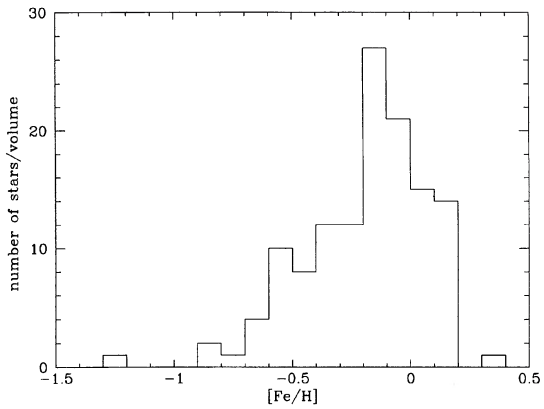

FIG. 3. Metallicity distribution of all local F/G dwarfs selected from the cross correlation of the Gliese and Olsen catalogs, plus the Sun.

turnoff after only 9 Gyr, the 12 Gyr turnoff color for this metallicity should be at least as red as the Sun, lending credibility to the interpolated value for solar metallicity obtained here. Accepting the solar metallicity 12 Gyr turnoff parameters based on the 1985 VandenBerg models, then the Edvardsson *et al.* trend predicts that the 12 Gyr turnoff color for a population of metallicity equal to +0.5 dex should be $(b-y)_{+0.5}=0.419$. This is also given for convenience in Table 2.

Figure 4(a) shows the raw sample of Gliese F/G stars plotted in the $[c_1-(b-y)]$ plane, together with the 12 Gyr turnoff colors for the relevant range of metallicities. All stars blueward of the turnoff for their metallicity (linear interpolation was used between fiducial points in the turnoff-color–[Fe/H] relation) are excluded from further consideration, since they occupy a region in which it is possible that old stars would have evolved out of the sample. Photometric errors are thus assumed to be unbiased. It should be noted that the Sun is excluded by this procedure; as noted above this is not unexpected, given that the main-sequence lifetime

TABLE 2. Adjusted turnoff $(b-y)$ colors.

[Fe/H]	$(b-y)$
−2.27	0.241
−1.77	0.260
−1.27	0.288
−0.79	0.323
−0.49	0.348
0.0	0.406
+0.50[a]	0.513
+0.50[b]	0.419

Notes to Table 2 :

(*a*) Interpolation in Table 1 of vandenBerg and Bell

(*b*) Predicted from Edvardsson *et al.*

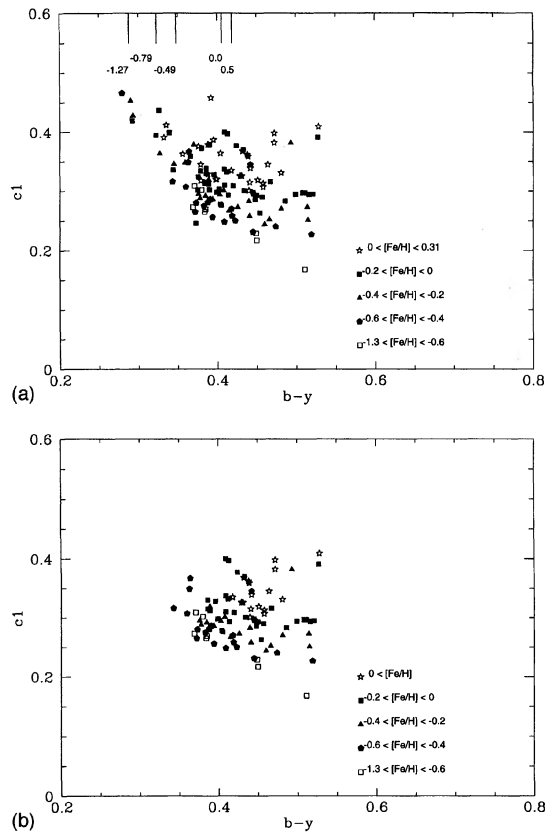

FIG. 4. (a) The sample of Fig. 3 in the $c_1-(b-y)$ plane, together with turnoff points for a range of metallicities, as described in the text. (b) The local sample after removal of stars expected to have main-sequence lifetimes shorter than the age of the disk.

of the Sun in these models is only 9 Gyr, which is less than our adopted age of the disk. For the stars of metallicity greater than the solar value, adopting the Edvardsson *et al.* turnoff color excludes only three fewer stars than does use of the redder vandenBerg and Laskarides turnoff color. In the following, we will use the results from adoption of the Edvardsson *et al.* color, since it is observationally calibrated.

The excluded stars from the Gliese catalog, which total 36 (plus the Sun), are indicated as such in Table 1 by a 'yes' in the column headed 'rejected?'. The sample remaining after this pruning, which totals 91 stars, has the color distribution shown in Fig. 4(b). The metallicity histogram corresponding to this 'G-dwarf' sample, is given in Fig. 5. This is our final metallicity distribution of long-lived stars observed in the solar neighborhood. This distribution will be combined with our metallicity distribution for long-lived stars *in situ* several kiloparsecs below the Galactic plane in the following sections. Given that our main scientific conclusions will be based upon comparing observations with observations, rather than comparing observations with precise theoretical predictions, we will not attempt any deconvolution of observational uncertainties from our metallicity distributions. Indeed, below we will rather rebin the local sample to match the (larger) uncertainties of the *in situ* data, ~0.2 dex.

A comparison of the distributions in Figs. 3 and 5 reveals

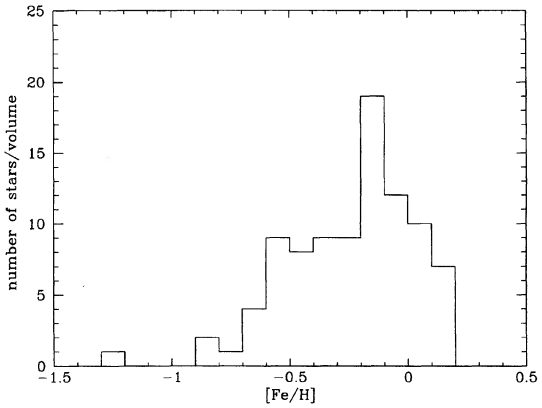

FIG. 5. Metallicity distribution of the local sample after the removal of short-lived stars.

that stars more metal-rich than [Fe/H]~−0.4 dex are preferentially removed. A consistency check on the robustness of our rejection of these stars may be made by comparison with two other samples. The first of these is the sample of around seven hundred K giants in the solar neighborhood of McWilliam (1990); these stars, being evolved, are by definition comparable to those stars rejected from our sample of long-lived F/G dwarfs. His sample contains every evolved G and K star in the *Bright Star Catalog*, and is approximately volume complete, but with a bias to higher mass, more distant stars. His abundance estimates are based on high-resolution spectra. The second sample consists of the F/G stars from the Edvardsson *et al.* (1993) sample that are younger than 12 Gyr, our chosen cutoff main-sequence life-time. Edvardsson *et al.* calculate the corrections required to generate a volume-complete metallicity distribution from their observed distributions. The metallicity distributions of these three samples—those stars rejected by our lifetime criterion (thus containing stars of all ages up to 12 Gyr), the local G/K giants (McWilliam 1990) and the volume-corrected Edvardsson *et al.* younger subsample—are shown together in Fig. 6. Note that we have chosen a wider bin size, 0.2 dex, to ensure

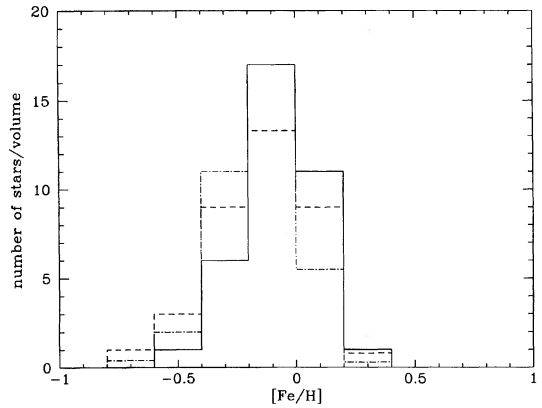

FIG. 6. Histograms of the iron abundance distributions for the Edvardsson *et al.* sample with ages less than 12 Gyr, after corrections for completeness (dashed lines); the McWilliam local G/K giant sample (dot–dashed lines) and the present sample of long-lived F/G dwarfs from the Gliese catalog (solid lines).

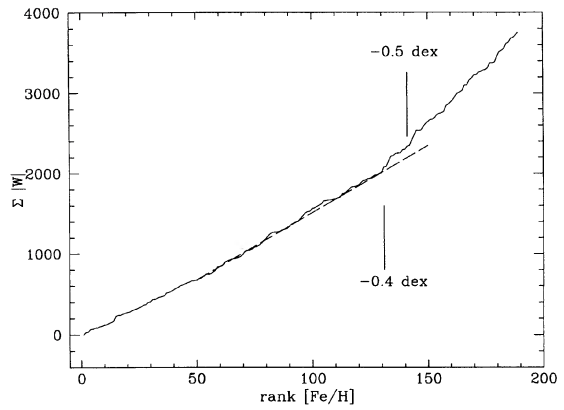

FIG. 7. [Fe/H] rank vs absolute value of the vertical velocity for the Edvardsson *et al.* sample, following Freeman (1991). The straight dashed line has been drawn to illustrate the change in kinematics.

that any small zero-point or scale differences which may exist between the different samples do not obscure the main point of the comparison. It is clear that the three distributions are all consistent with one another, and provide a well-defined metallicity distribution function for the younger thin disk.

It should also be noted that even the VandenBerg (adjusted) 12 Gyr turnoff for a stellar population of three times solar metallicity, $(b-y)=0.513$, is bluer than the red limit of the data, $(b-y)=0.528$; this means that old, metal-rich stars have *not* been excluded by our selection procedures. This was not known to be the case for previous samples.

2.5 What Stars Have We Isolated?

The sample whose chemical abundance distribution we have obtained will be a mix of all the stellar populations that are represented in the solar neighborhood—effectively, the thick and thin disks. Kinematics are usually invoked to determine the boundary of the thick disk/thin disk transition. As exemplified by the analysis of Freeman (1991, 1994), the vertical velocity distribution of the Edvardsson *et al.* sample (which has no kinematic-metallicity bias) can be described by essentially two numbers $-\langle|W|\rangle$ approximately constant at 19 km s^{-1} for thin-disk stars, and $\langle|W|\rangle\simeq 42$ km s^{-1} for thick-disk stars. The value for the thin-disk stars is generally understood as reflecting the saturation of the disk-heating mechanism by scatterers confined to the disk plane (e.g., Lacey 1991). Freeman assigns age ranges to these kinematics, but one can also look at metallicity ranges. Following his approach, Fig. 7 shows the cumulative $|W|$ velocity against [Fe/H] rank for the Edvardsson *et al.* sample; in such a plot a straight line has a slope equal to the mean of the absolute value of the W velocity; this is an approximation to the dispersion if the underlying distribution function is a single zero-mean Gaussian.

It is clearly consistent with the data to adopt the colder kinematics (indicated by the dashed line) for the stars more metal rich than [Fe/H]~ -0.4 dex, whereas the hotter component is evidently present in those stars with $-1.0\leqslant$[Fe/H]<-0.4. Thus, purely kinematic definitions show the thick disk to be an important component of the disk for stars with metallicity below [Fe/H]<-0.4. We now check to see if it is a dominant or even unique component.

Figure 5 above is the abundance distribution function for our final local sample. Simple counting shows that the fraction of the sample which has abundance below [Fe/H]<-0.4 is $\gtrsim$25%, and below [Fe/H]<-0.5 is $\lesssim$20%. This can be compared with that derived from star-count models, which reproduce the number of stars *in situ* some 1–2 kpc from the Galactic plane, using a (highly correlated) combination of a scale height and a local volume density, expressed as the ratio of thick-disk to thin-disk stars. Typical star-count models provide estimates of this local ratio of thick-disk to thin-disk stars of between $\sim$2% and $\sim$10%, with the most recent models being in the middle of this range (Gilmore *et al.* 1989; Majewski 1993; Ojha *et al.* 1994, and references therein). That is, with this metallicity identification of the thick disk, which is apparently consistent with kinematic data, there is an apparent *overdensity* of thick-disk stars in the local sample here by a factor of about 5. Thus there is a serious failing of at least one of the star-count models, the bivariate definition of the boundary between the thick and the thin disks, or of the assumption that the thick-disk–thin-disk boundary is discontinuous.

The star-count models are sufficiently successful that the possibility they are in error by the required magnitude can be excluded. The bivariate kinematics-chemistry determination of the *onset* of the thick disk is justified above. Thus we must deduce that there is a substantial overlap between the thick disk and the thin disk. That is, the onset of the thick disk, as evidenced in the rapid change in vertical velocity distribution (Fig. 7) at a metallicity of [Fe/H]~ -0.4, does not correspond to the end of the thin disk. This interpretation requires that the vertical velocity distribution function for these lower metallicity stars is not a single Gaussian.

The composite nature of the velocity distribution is confirmed in Figs. 8(a)–8(d), which show histograms of the vertical velocity data for all the Edvardsson *et al.* stars [panels (a) and (c)] and all the single Gliese F/G dwarfs [panels (b) and (d)], with metallicity in the range $-0.4\leqslant$[Fe/H]<-0.9 [panels (a) and (b)] and with metallicity in the range $-0.5\leqslant$[Fe/H]<-0.9 [panels (c) and (d)] (W velocities for these stars are listed in Table 1; we note that there is only one metal-poor star—HD 100004—that was rejected from our potentially long-lived sample and which is in this complete sample). The smooth curve superposed corresponds to a Gaussian with dispersion of 45 km s^{-1}; there is evidently a cold core, reminiscent of the thin-disk kinematics, in addition to the stars with hotter, thick-disk kinematics. This cold core persists even after the exclusion of stars in the range $-0.4\leqslant$[Fe/H]<-0.5. Note that we are limited, by the small sample sizes, to this broad a metallicity range, and so are unable from these data alone to determine the true detailed metallicity distribution of local stars with thin-disk kinematics, but can say that it clearly extends into the regime of the thick disk. In contrast, stars with thick-disk kinematics are not a substantial contributor at higher metallicities, [Fe/H] $\gtrsim -0.3$, or they would be visible in Fig. 7. We achieve the deconvolution of the thick-disk and thin-disk metallicity dis-

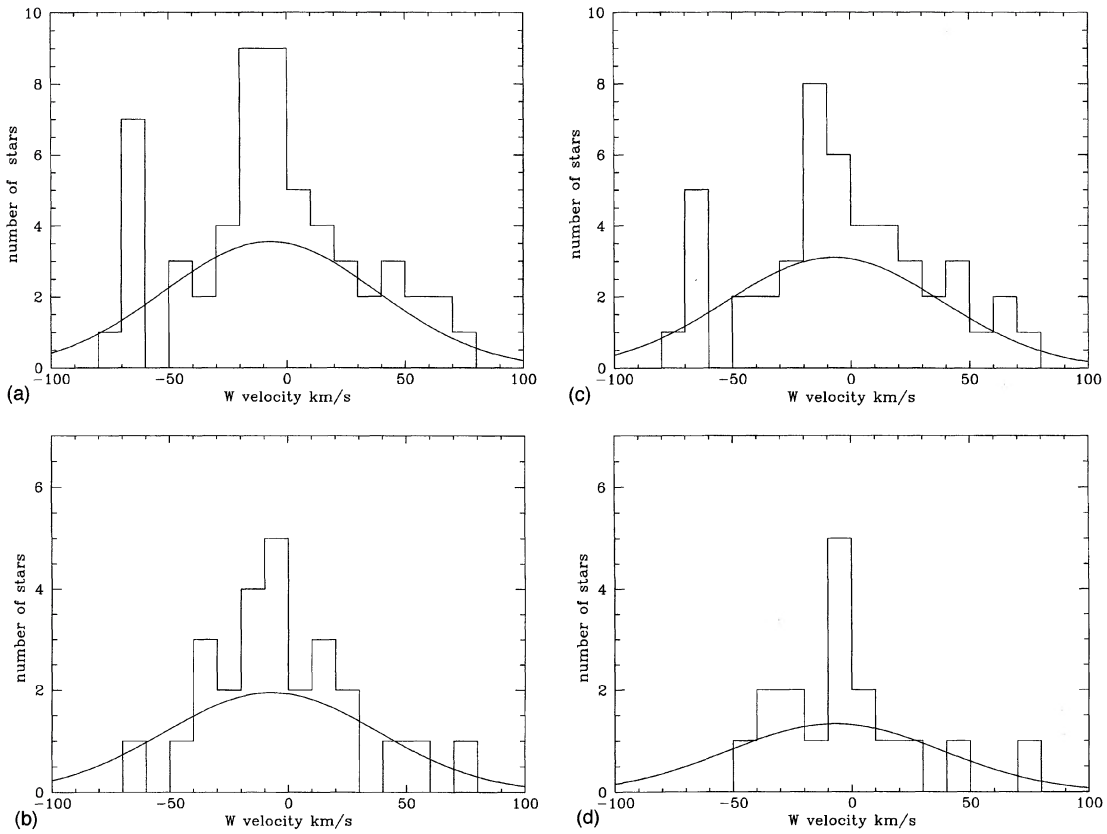

FIG. 8. (a) Histogram of the W-velocity data for the subsample of the Edvardsson *et al.* stars with iron abundance in the range $-0.4 \geqslant [Fe/H] > -0.9$, where naively one might have expected the thick disk to dominate. The smooth curve is a Gaussian of dispersion 45 km/s^{-1}, normalized by eye. (b) As (a), but for the complete sample of Gliese F/G dwarfs. (c) As (a), but for the more metal-poor stars, with iron abundance in the range $-0.5 \geqslant [Fe/H] > -0.9$. (d) As (b), but for the more metal-poor stars, with iron abundance in the range $-0.5 \geqslant [Fe/H] > -0.9$.

tributions in Sec. 3 below, by combining distant and local data.

The fact that thin-disk stars are significant, if not dominant, contributors to the metallicity distribution at [Fe/H] ~ -0.6, around the peak of the thick-disk metallicity distribution, results from the much higher local normalization of thin-disk stars. As discussed by Gilmore & Wyse (1985), the old thin disk has a characteristic value in its metallicity distribution of [Fe/H] ~ -0.25, and a width which may be characterized crudely by a Gaussian of dispersion 0.2 dex. This combination of a higher local normalization and a peak at a metallicity which is only as far as the spread of its distribution from the maximum of the thick-disk distribution, means that a large part of the metal-poor local stellar populations are members of the thin disk. We return to this point in Sec. *3.2* below.

3. THE SOLAR CYLINDER G-DWARF METALLICITY DISTRIBUTION

We have identified above a reliable and volume-complete, though small, local sample of potentially long-lived stars. We recall that any such sample in the Plane may undersample high velocity dispersion components of the disks, and so should be corrected accordingly. Conversion of this sample into a fair estimator of the local time-integrated chemical abundance distribution requires that this sample be corrected from volume to surface density. The simplest models of galaxy evolution assume there is no *radial* rearrangement of chemically enriched material, with vertical and radial kinematics decoupled, so that one should integrate in a column perpendicular to the disk. This may be achieved either by kinematic weighting of a local sample, or by interpolating between a local and a similar distant *in situ* sample. This second approach, achieved for the first time in this paper, has the additional benefit that the comparison may be used to estimate more reliably than was possible above the relative contributions of low velocity dispersion (thin-disk) and high velocity dispersion (thick-disk) stars to the metal-poor stellar distribution. We address both options in this section.

3.1 Kinematic Weighting of the Local Sample

We now attempt to define a representative metallicity distribution function from our local stellar sample using a kinematic-dependent weighting. This is to correct for the fact that the probability of observing a star on a given orbit while it is in the solar neighborhood depends on the fraction of the orbit that the star spends there. It also provides for the transformation of volume densities to surface densities, leading to

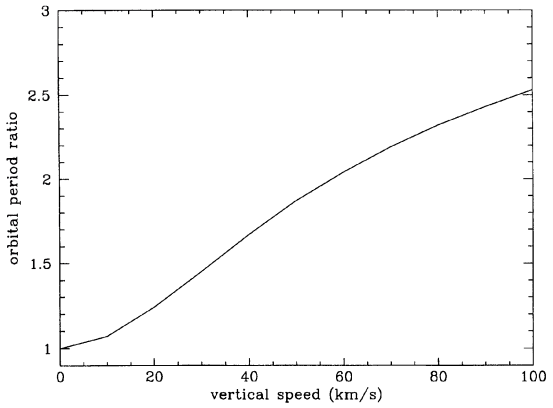

FIG. 9. Ratio of the vertical orbital period in the actual Galactic potential to that in an harmonic potential, as a function of vertical velocity at the disk plane.

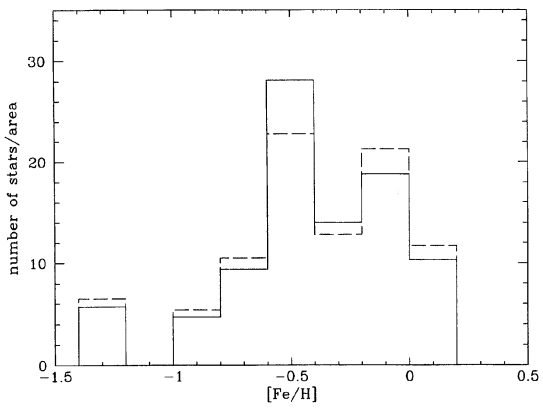

FIG. 11. Iron abundance distribution of the local sample after the weighting to account for kinematic bias.

the iron abundance distribution integrated through the solar cylinder. The correction factor is the inverse of the fraction of an orbit that a star spends traversing the disk, and thus is proportional to the product of the vertical speed passing through the plane, $|W_{z=0}|$, and the vertical oscillation period for that star's orbit. The vertical period should be calculated from the measured vertical potential gradient of the Galactic disk rather than from an harmonic potential approximation (which has constant vertical period). Figure 9 shows the relation between oscillation period and vertical speed that results from the vertical force law derived by Kuijken & Gilmore (1989). This was adopted here.

In principle, the correction could be done on a star-by-star basis, using the space motions in the Gliese catalog. However, the small sample size, 91 stars after pruning, leaves this procedure susceptible to sampling errors. A more robust weighting is that derived from the best available estimator of the true vertical velocity dispersion appropriate for a specific abundance range, provided that one knows reliably the relative fractions of stars in that specific abundance range which are thin disk and thick disk. As emphasized earlier, this information is not available *a priori*. Thus weightings of this type are inherently unreliable. However, to compare with previous analyses we go through such a weighting exercise here.

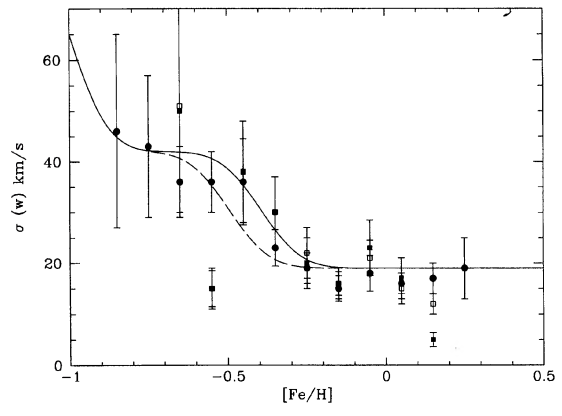

FIG. 10. Vertical velocity dispersion as a function of iron abundance for the Gliese catalog stars and the F/G star sample of Edvardsson *et al.* (1993). The filled square symbols refer to the 'raw' Gliese sample, the open squares to that obtained subsequent to pruning of potentially short-lived stars, and the filled circles to the Edvardsson *et al.* sample. The error bars are appropriate for an underlying Gaussian distribution. The solid line is the result of convolving a Gaussian of dispersion 0.1 dex with the step-function velocity-dispersion–metallicity relation suggested by the data.

The vertical velocity dispersion as a function of iron abundance for the Gliese catalog sample—both the 'raw' sample and that obtained subsequent to pruning of potentially short-lived stars—together with that of the local F/G star sample of Edvardsson *et al.* (1993) is shown in Fig. 10. The solid curve is the result of convolving a step-function relationship between velocity dispersion and [Fe/H], with the transition between a velocity dispersion of 19 to 42 km s^{-1} at −0.4 dex, as suggested by Fig. 7, with a Gaussian of dispersion 0.1 dex, the expected metallicity accuracy. The smooth dashed curve results from adopting a value of −0.5 dex for the transition metallicity, and serves as an estimate of the uncertainty introduced by this approach. These smooth relationships were used to assign a velocity dispersion to each metallicity bin of the present sample, rebinned into 0.2 dex wide bins. The kinematic corrections were thus effected by weighting the binned data (after evolutionary corrections) by the product of the vertical velocity dispersion of that bin, times the extra factor due to the period lengthening in a nonharmonic potential (from Fig. 9), adopting the velocity dispersion as the estimator for the relevant mean vertical speed; this is justified for *relative* weighting.[3] The resulting metallicity distribution was then renormalized to the same number of stars, for convenience. This procedure resulted in the metallicity distribution of Fig. 11, where the solid and dashed histograms correspond to the adopted kinematics in the weighting scheme indicated by the solid and dashed curves in Fig. 10. One should remember that the kinematic weighting assumes that all stars more metal poor than −0.4

[3]Note also that using our procedure with the adopted velocity dispersions of Sommer-Larsen (1991) resulted in a weighting factor that is numerically equal (to within a few percent) to that obtained by Sommer-Larsen by his more indirect technique.

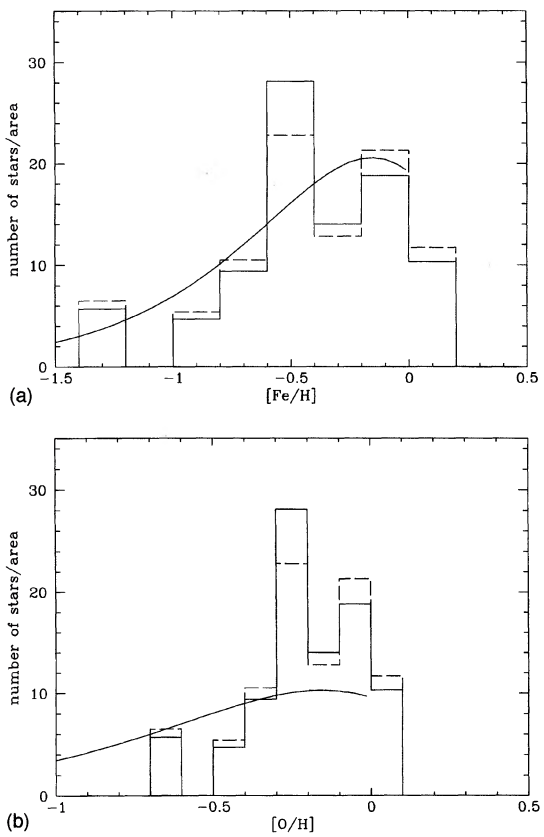

FIG. 12. (a) As Fig. 11 but with the predictions of a 'simple closed-box' model of yield $0.7Z_{\odot}$, and present gas fraction 0.25, truncated at the metallicity corresponding to these values and normalized to the total number of stars in the sample. (b) As (a), but for the transformed 'oxygen' metallicity distribution.

dex (or −0.5 dex) belong to a single population, with kinematics characterized by a simple, single Gaussian; this is a dubious assumption.

The metallicity distributions of Fig. 11 do not differ radically from earlier determinations. There are somewhat fewer stars below [Fe/H]~ -0.7 dex than have the distributions resulting from Cameron's (1985) UV excess calibration from broadband *UBV* photometry (Pagel 1989; Sommer-Larsen 1991); as we have noted, this metallicity calibration provides systematically lower [Fe/H] estimates than, e.g., that of Carney (1979), while the larger errors of the UV excess technique will broaden the distribution. After weighting, the present sample has relatively fewer stars above solar metallicity than does either of the Pagel distributions, but is similar to that of Sommer-Larsen. The fraction of stars more metal poor than −0.4 dex is approximately 45%.

For interest, to compare with previous results, we show in Fig. 12(a) these same distributions, with an overlaid Simple Model of yield 0.7 solar abundance, and evolved to a gas fraction of 0.25, as appropriate for the local disk (Kuijken & Gilmore 1989). While the model could not be described as providing an excellent description of the data, the discrepancies are not overwhelming. As we emphasize below, however, we explicitly do not suggest that this model is a viable representation of these data, nor that the distribution function of Fig. 12(a) is that appropriate to the local Galactic disk. Indeed, the possible traps for the unwary may be illustrated by, following Pagel (1989), transforming the iron abundance distribution into one for oxygen. The Simple Model predictions are based on the instantaneous recycling approximation, and as such are better compared to metallicity distributions based on elements that are produced predominantly by massive stars, such as oxygen, rather than the iron-based distribution usually measured (cf. Pagel 1989). As discussed above, for most of the stars of interest, with [Fe/H]$\gtrsim -1$ dex, the simple relationship [O/H]$= -0.5$[Fe/H] is a reasonable approximation (e.g., Edvardsson *et al.* 1993). Using this to transform an iron distribution into an oxygen distribution simply squashes the metallicity scale of the observations. The resulting distribution and Simple Model are shown in Fig. 12(b); it is much clearer now that the Simple Model distribution is significantly *wider* than the observations.[4]

3.2 Comparison to the in situ Sample

Gilmore *et al.* (1995) determined the iron abundance distribution of G dwarfs at several kpc above the Galactic plane. Those distributions were derived from spectroscopic observations of area-complete, photometrically defined samples of F/G dwarfs in the apparent magnitude range $16 \lesssim V \lesssim 18$. The final distribution of stars *per unit volume* at a chosen fiducial distance depends on the density law assumed for the stars. Figure 19 from that paper is reproduced here as Fig. 13, showing the iron abundance distributions at $z = 1.5$ kpc in the direction of the South Galactic Pole and at $z = 1$ kpc in a field at ($l = 270$, $b = -45$), UK Schmidt F117; for the magnitude range under study these two lines-of-sight probe essentially the same Galactocentric distance projected on the plane. The distributions shown are derived under two sets of assumed density laws; in one case that all the stars are thick-disk stars, and in the other case that the stars more metal poor than [Fe/H]$= -1.0$ are halo objects, while the stars more metal rich than [Fe/H]$= -0.4$ are 90% thick-disk and 10% thin-disk stars (a ratio consistent with star-count model predictions at the sample distance from the Galactic plane) and 100% thin disk for [Fe/H]> 0.0. Adopted vertical scale heights were 4000 pc for the halo, 1000 pc for the thick disk, and 250 pc for the thin disk, in agreement with the adopted velocity dispersions and vertical potential above. Full details are provided in Gilmore *et al.* (1995).

The metal-rich bins are expected to be under-represented, since the sample was selected *in situ*, far from the Galactic plane, requiring a high minimum vertical velocity at the plane, for a given star. Metal-rich stars in general may be expected to be drawn from a population with vertical velocity dispersion of only ~ 20 km s^{-1} (Edvardsson *et al.* 1993;

[4]It should be noted that the gas fraction appropriate to the solar circle, 0.25, is rather higher than had been adopted in the past; this larger value results in the truncation of the model evolution at metallicities below the extent of the data, for yields that approximate the location of the peak in the observational data. The main input parameters to the local gas fraction whose values have been reestimated recently are the actual gas surface densities, and the total disk surface density (see Kuijken & Gilmore 1989).

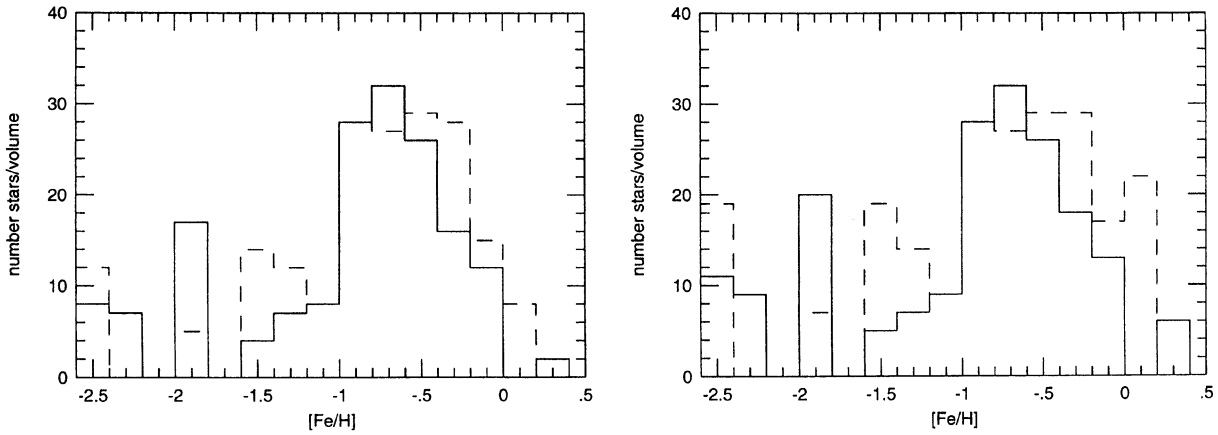

FIG. 13. Figure 19 from Gilmore *et al.* (1995). Comparison of the F117 $z=1000$ pc iron abundance distribution (solid histograms) and the SGP $z=1500$ pc distribution (dashed histograms). The left panel shows the derived distributions under the assumption that all stars follow the thick-disk density profile, while the right panel includes thin-disk and stellar halo contributions.

Freeman 1991), so that only stars in the tail of the velocity distribution will be sampled *in situ* at a few kpc. That is, this sample suffers from the complementary selection bias to that suffered by the nearby-star sample, systematically undersampling low velocity-dispersion populations. Indeed, there is *no* significant dependence of the observed line-of-sight velocity dispersion on metallicity for either the SGP stars (typical dispersion is $\sigma_W \sim 40$ km s^{-1}), or the F117 stars (typical dispersion is $\sigma_{los} \sim 50$ km s^{-1}; Gilmore and Wyse, in preparation), suggesting that the colder thin-disk stars are indeed relatively undersampled. We can use this kinematic bias to determine the number of low vertical velocity, metal-poor stars in the local sample.

The predicted distribution at $z=0$ pc may be derived from these data, again once an appropriate choice of density law is made. Obviously the case where all stars are thick-disk stars, and so each metallicity bin is corrected using the same density profile, will have the same relative distribution as that shown in Fig. 13, with only the overall normalization increased. The distributions obtained under the alternative assumption, that the metal-poor bins are dominated by halo stars, while the metal-rich bins are dominated by thin-disk stars, are shown in Fig. 14. It should be noted that the original sample has very few stars at either extreme in metallicity.

The two lines of sight provide independent probes of the *in situ* metallicity distribution, with approximately equal numbers of stars in the original samples, and in each bin, and so a composite distribution may be obtained by a simple unweighted sum.

The distributions shown are most reliable in the range of $-1 \lesssim [Fe/H] \lesssim -0.2$, where we have most stars in the original sample, and for which the iron-abundance estimator is most robust (see Jones *et al.* 1995a; Jones *et al.* 1995b; Gilmore *et al.* 1995 for details). This is also the range of metallicity for which there is minimal difference between the two treatments of the density law(s). Comparing to the unweighted Gliese sample of Fig. 5, the *in situ* sample at the plane has a rather different distribution for metal-poor stars, being flat from [Fe/H]~ -0.5 to [Fe/H]~ -1 dex. The difference in distributions between the local sample and the *in situ* sample brought down to the plane is due to the presence of those kinematically cold stars in the local sample with metallicity $[Fe/H] \lesssim -0.4$. Thus comparison of these two samples thus allows us to deduce the shape of the thin disk metallicity distribution below its peak.

The distributions functions must first be matched: this should be at an iron abundance where the thick disk may reasonably be expected to dominate, rather than just be present as a small minority population. An independent estimate of this abundance may be made by inspection of the age–metallicity–kinematics relations of Edvardsson *et al.* (1993) and of Marquez & Schuster (1994). These show that, although there is a substantial scatter in the thin disk age–abundance relationship, there is no significant population of stars with $[Fe/H] \lesssim -0.7$ dex that is younger than 12 Gyr, or has kinematics cooler than those of the thick disk. The stellar halo, on the other hand, dominates for $[Fe/H] \lesssim -1$ dex (Marquez & Schuster 1994). Thus, we match the *in situ* sample,

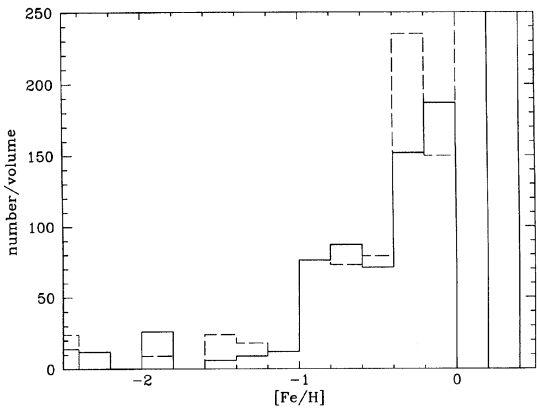

FIG. 14. The $z=0$ pc iron abundance distribution resulting from the *in situ* data, if density laws appropriate to the halo are assumed for the metal-poor stars, and that appropriate to the thin disk for the most metal-rich stars, as described in the text.

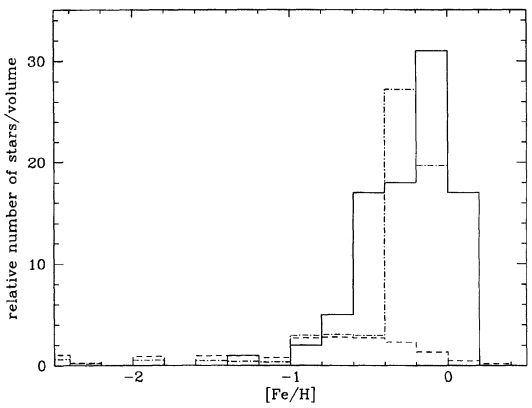

FIG. 15. The solar neighborhood iron abundance distribution that results from matching the *in situ* data, brought to the Plane, to the local data, as described in the text. The dashed lines denote the $z=0$ pc, formerly *in situ*, distribution, assuming all stars are thick-disk stars; the dash–dotted curve is the comparable distribution adopting the three-component scaling—both now renormalized to match, over the interval $-0.8>$[Fe/H]>-1 dex, the solid histogram, which represents the local Gliese long-lived F/G dwarf sample. The *in situ* data have been truncated at solar metallicity.

scaled to the plane, and the local sample, over the interval $-0.7>$[Fe/H]>-1 dex. Further, both distributions should be reliable here. We carry out this matching for both scalings to the plane, that assuming that all stars at $z=1500$ pc are thick-disk stars, and that assuming the three-component distribution in the *in situ* sample. The uncertainties in the iron abundance estimates of the *in situ* sample are around 0.2 dex; the local sample was rebinned to this prior to the matching.

In view of the small number statistics in the local sample at low abundances, we proceed by adopting the *shape* of the thick-disk chemical abundance distribution function as derived from the scaled *in situ* sample. Given that *shape*, we normalize the counts iteratively to provide a self-consistent match to the local metal-poor abundance distribution and the kinematic distributions shown earlier. That is, the normalization of the thick-disk distribution function is derived by allocating a subset of those stars in the abundance range $-0.8<$[Fe/H]<-0.4 to the thick disk, with the *relative* numbers from each abundance bin determined by the adopted shape for the thick-disk distribution. The normalization is derived from the combination of the kinematics of Fig. 9 and the (small) number of stars in the chemical abundance range $-1.0<$[Fe/H]<-0.8, which is assumed pure thick disk.

This matching results in the histograms shown in Fig. 15. The dashed lines denote the $z=0$ pc, formerly *in situ*, distribution, assuming all stars are thick-disk stars; the dash–dotted curve is the comparable distribution adopting the three-component scaling, as defined above—both now renormalized as above to match the solid histogram, which represents the local Gliese long-lived F/G dwarf sample. While the normalization is imprecise in consequence of small-number statistics, it is clear that, with either assumption in renormalizing the *in situ* sample, there is a considerable excess group of stars with [Fe/H]~-0.5 in the local Gliese sample, compared to the number in the other distributions. It is also apparent that there is reasonable agreement between the renormalized *in situ* sample, after scaling to the plane, in the number of stars with $-0.4\leq$[Fe/H]≤ 0.0, although the detailed shape of the distribution function remains uncertain, *only* if the three-kinematic component model is adopted. We note that it is this model which is also consistent with star-count models (Gilmore *et al.* 1995).

That is, a matching of the local volume-complete sample of long-lived F/G dwarfs with a comparable sample, selected near 1500 pc from the Sun, and corrected through density profiles and normalizations consistent with kinematic and star-count data, requires that a majority of the stars near the Sun with [Fe/H] near -0.5 dex have kinematics appropriate to the thin disk and not the thick disk. This population may extend, but only as a minority constituent, to at least [Fe/H] ≈-0.8. Similarly, it is probable that some stars with thick-disk kinematics extend upwards in metallicity to [Fe/H] ≈-0.2 dex. It is this overlap of populations which resolves the apparent inconsistency between star-count models, which require the local thick-disk normalization in a volume-complete sample to be a few percent, and the abundance distribution of the local volume-complete (Gliese catalog) samples, where metal-poor stars comprise some 25 percent of the total.

In summary, from this deconvolution, we now derive an abundance distribution for the long-lived stars of the Galactic disk by assigning the stars with $-0.8<$[Fe/H]≤-0.6 to populations with vertical velocity dispersions of 42 and 19 km s^{-1} (Freeman 1991) in the ratio of 3:2; those in the interval $-0.6<$[Fe/H]≤-0.4 in the ratio 1:5; and those in the interval $-0.4<$[Fe/H]≤-0.2 in the ratio 1:10. With these kinematic assignments, we are able to derive a column-integral abundance distribution, utilizing the weightings of Fig. 9 above.

For completeness, we also recall the results of Wyse & Gilmore (1992) and of Ibata & Gilmore (1995), which show that the angular momentum distributions of the halo and the inner bulge are indistinguishable from each other, but are very different from those of the thick disk or the thin disk, which are in turn indistinguishable from each other. Thus, those studies conclude that the halo–bulge system of the Galaxy is a parallel evolutionary sequence to that of the thick disk–thin disk. We summarize all these results in Fig. 16. This shows the (normalized to unity for each distribution) abundance distribution of the Solar neighborhood halo (Laird *et al.* 1988), the outer Galactic bulge (Ibata & Gilmore 1995), the younger stars of the solar neighborhood, from Fig. 6 above, the volume complete sample of long-lived thin-disk stars, derived here from our composite Gliese and scaled *in situ* samples, the (similarly derived) volume complete sample of local thick-disk stars, and the column-integral summed abundance distribution for the long-lived thin disk and the thick disk derived here from those latter two distributions. The six distributions are also presented, for convenience, in Table 3.

4. DISCUSSION

A variety of distribution functions relevant to the evolution of the Galactic disk, and in particular to the question of the stellar population structure in the Galactic disks, have

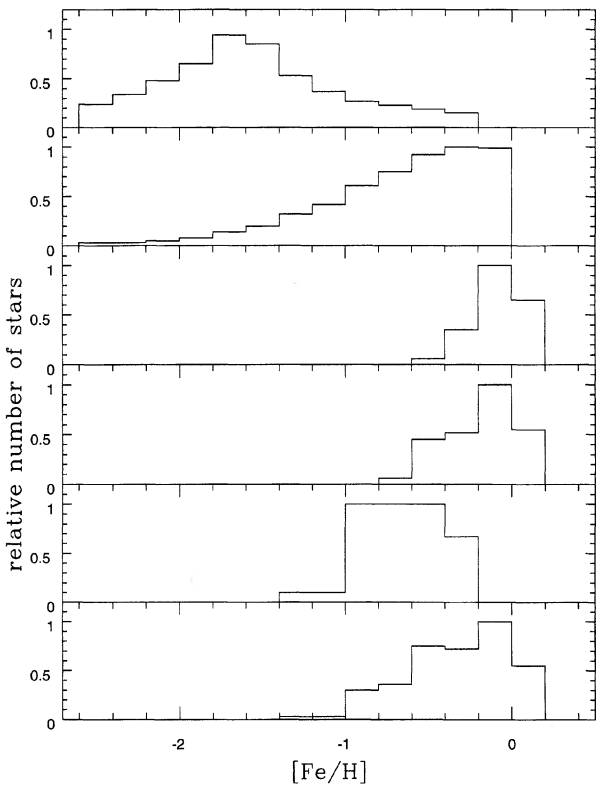

FIG. 16. Abundance distributions, normalized to unity, of, from top to bottom, the Solar neighborhood halo (Laird *et al.* 1988); the outer Galactic bulge (Ibata & Gilmore 1995), truncated by them at solar metallicity; the younger stars of the solar neighborhood, from Fig. 6 above; the volume complete sample of long-lived thin-disk stars, derived here from our composite Gliese and scaled *in situ* samples; the (similarly derived) volume complete sample of local thick-disk stars; and the column-integral abundance distribution for the sum of the long-lived thin disk and the thick disk, derived here from those latter two distributions.

become reliably defined in the last few years. Among the most important of these have been determinations of the age–metallicity–kinematics distribution of F/G stars in the Solar neighborhood. These have been complemented by many recent star-count and kinematic studies, which have determined reasonably reliable and precise normalizations for the three stellar populations evident in the Solar neighborhood data: the halo, the thick disk, and the thin disk. In this paper we have achieved a new derivation of the abundance distribution for the local, volume-complete sample of long-lived stars, using the most recent and precise photometry and calibrations. This determination, which is in general agreement with other recent such determinations, but more reliable, was demonstrated above to provide a local fraction of metal-poor stars which exceeds that derived from the larger-scale studies (star counts and *in situ* chemical abundance distributions) by a factor of about five. Comparison of the local abundance determination with that determined from two *in situ* samples, each some 1500 pc from the Sun, isolates the explanation of this inconsistency: a majority of the stars with metallicity near [Fe/H]≈ -0.5 dex in the Solar neighborhood have thin-disk kinematics. The apparent rather abrupt transition in kinematics near [Fe/H]≈ -0.4 dex, as in Fig. 7, is rather a confusing manifestation of two overlapping distribution functions. The combination of kinematics, spatial distribution, and chemical abundances for samples with different selection effects was required for this understanding.

The underlying metallicity distribution function for the old thin disk extends to at least [Fe/H]≈ -0.75 dex, and possibly to even lower abundances. Similarly, the thick-disk abundance distribution extends up to at least [Fe/H]≈ -0.3 dex, and possibly to even higher abundances. This overlap, while confusing simple analyses, is consistent with the observed scatter in recent age–metallicity relations, which show a significant number of stars with [Fe/H]$\lesssim -0.5$ dex, and with ages of only a few Gyr, and which are providing improving evidence for stars with [Fe/H]≈ 0, and with ages more typical of the bulk of the thick disk, some 12 Gyr [cf. Fig. 14(a) of Edvardsson *et al.* 1993]. It is clear that age distributions are are also going to provide important constraints on theories of disk evolution. Whether these are old, thin-disk stars or metal-rich thick-disk stars remains a matter for future investigations.

The result that the abundance distributions of the thick disk, which is apparently exclusively old, and of the thin disk overlap considerably, with the thin disk extending to abundances nearly as metal poor as does the thick disk, has implications for models of the formation of the thick disk. This is consistent with the simplest class of merger models for the formation of the thick disk only if there is substantial scatter in the age–metallicity relationship for thin-disk stars at all times, even during the earliest stages. In such models the thick disk is formed during the merger of a predominantly stellar satellite galaxy with an extant Galactic disk (e.g., Quinn *et al.* 1993). Dramatic kinematic heating of those thin-disk stars already formed abruptly thickens the thin disk into a thick disk, which will also contain much of the stellar population of the incoming merging galaxy. The remaining disk gas will rapidly restabilize into a new thin disk, and continue its evolution. The chemical evolution is relatively unaffected by the merger, and the first newly forming thin-disk stars will have the mean metallicity which the interstellar medium had attained prior to the merger, which will be greater than the mean abundance of the stars in the newly thickened disk. In this class of model, substantial overlap in abundances is not a natural feature without appeal to large scatter in the age–metallicity relationship of those stars formed prior to the merger, as well as those formed after.

As part of the present analysis, we have isolated, in order to remove from our complete sample of long-lived stars, the distribution of abundances of younger stars near the Sun. This distribution is more metal rich in the mean, and is skewed to higher abundances, than is the distribution of abundances of longer-lived stars, which will in the mean be older. Thus, there is a trend of abundance with age in the Galactic disk. Remarkably, however, there appears to have been little or no change in the mean abundance of the old disk in the interval between about 10 Gyr ago and about 3 Gyr ago. In the last few Gyr the mean iron abundance has increased by a factor of about two, while the tail of the thin-disk abundance distribution to metal-poor stars has dis-

TABLE 3. Abundance distribution functions for stellar populations.

[Fe/H]	Field Halo	Outer Bulge	Young Disk	Thin Disk Volume	Thick Disk Volume	Thin + Thick Column
	Note 1	Note 2	Note 3	Note 4	Note 4	Note 5
+0.3	–	–	–	–	–	–
+0.1	–	–	0.65	0.55	–	0.55
−0.1	0.00	0.99	1.00	1.00	0.00:	1.00
−0.3	0.15	1.00	0.35	0.52	0.67	0.72
−0.5	0.19	0.92	0.06	0.45	1.00	0.75
−0.7	0.23	0.75	0.00	0.06	1.00	0.36
−0.9	0.27	0.61	0.00	0.00	1.00	0.30
−1.1	0.37	0.42	0.00	0.00	0.10:	0.03
−1.3	0.53	0.32	0.00	0.00	0.10:	0.03:
−1.5	0.85	0.20	0.00	0.00	0.00	0.00
−1.7	0.94	0.14	0.00	0.00	0.00	0.00
−1.9	0.65	0.08	0.00	0.00	0.00	0.00
−2.1	0.48	0.08:	0.00	0.00	0.00	0.00
−2.3	0.34	0.03:	0.00	0.00	0.00	0.00
−2.5	0.24	0.03:	0.00	0.00	0.00	0.00

Notes to Table 3:

Note 1: data from Laird *et al* (1988).

Note 2: data from Ibata and Gilmore (1995).

Note 3: Gliese pruned stars, this paper.

Note 4: This paper, §3.

Note 5: This paper. Weights (from Figure 9) are, for isothermal samples with vertical dispersions 42km/s and 19km/s, in the ratio 3.09.

appeared. This conclusion from the present analysis is consistent with the age–metallicity–kinematic data of Edvardsson *et al.* (1993), which show a turn-up in the mean chemical abundance within the last few Gyr [their Fig. 14(a)].

Identification of a large fraction of the metal-poor [Fe/H]$\sim$−0.5, stars in the Solar neighborhood with the thin disk, so that their kinematics confine them close to the disk plane, means that recent attempts (including those by ourselves in Sec. *3.1* above) to derive the column-integral abundance distribution near the Sun by kinematic-weighting of the local data will *over-estimate* the true number of metal-poor stars in the Galactic disk. This arises since the practice has been to identify all metal-poor stars with the thick disk, and thus necessarily use thick-disk kinematics in the weighting applied to all these stars. Figure 8 demonstrated the danger of assuming a simple single Gaussian fit to determine the kinematics appropriate to a given sample. Hence, to use the jargon of the Simple Model of chemical evolution, the 'G-dwarf problem' seen in the fitting of the solar cylinder data is even more severe than has been suggested recently, since the true contribution of metal-poor stars to the column integral has been overestimated in the past by the simple kinematic weighting procedure which had been adopted. We emphasize, however, that the assumptions underlying the Simple Model are inappropriate to the evolution of a part of a galactic disk, so that this deduction by itself is not a very helpful clue to improve models of galactic evolution.

A variety of recent studies have provided a determination of the Solar cylinder chemical abundance distribution taking account of local kinematics. In this study we have included data for distant stellar samples, allowing a more robust deconvolution of the high-precision, but small sample, local data than has been possible heretofore. Such abundance determinations are useful constraints on Galactic chemical evo-

lution, but contain insufficient information for detailed analysis. Further progress requires consideration of the multivariate distribution function, complementing the results of this study with both age and chemical element ratio information.

We thank the referee, Bernard Pagel, for helpful suggestions which have improved the presentation. R.F.G.W. acknowledges support from the AAS Small Research Grants Program in the form of a grant from NASA administered by the AAS, from the NSF (AST-9016226) and from the Seaver Foundation. Our collaboration was aided by NATO Scientific Affairs in the very early stages and currently by the NSF (INT-9113306). NSSDC provided necessary access to data catalogs. The Center for Particle Astrophysics is supported by the NSF.

REFERENCES

Aguilar, L., Carney, B., Latham, D., & Laird, J. 1995, in preparation
Cameron, L. M. 1985, A&A, 146, 59
Carney, B. W., 1979, ApJ, 233, 211
Carney, B. W., Latham, D. L., & Laird, J. 1989, AJ, 97, 423
Crawford, D. L., & Barnes, J. V. 1969, AJ, 74, 407
Edmunds, M. G. 1990, MNRAS, 246, 678
Edvardsson, B., Andersen, J., Gustafsson, B., Lambert, D. L., Nissen, P., & Tomkin, J. 1993, A&A, 275, 101
Freeman, K. C. 1991, in Dynamics of Disc Galaxies, edited by B. Sundelius (Göteborgs University, Göteborg), p. 15
Freeman, K. C. 1994, in Dynamics of Disc Galaxies, special session at the AAS Summer meeting, 1994
Gilmore, G. 1990, The Milky Way as a Galaxy (University Science, Berkeley) edited by G. Gilmore, I. King, and P. C. van der Kruit
Gilmore, G., & Wyse, R. F. G. 1985, AJ, 90, 2015
Gilmore, G., & Wyse, R. F. G. 1986, Nature, 322, 806
Gilmore, G., Edvardsson, B., & Nissen, P. 1991, ApJ, 378, 17
Gilmore, G., Wyse, R. F. G., & Jones, J. B. 1995, AJ, 109, 1095
Gilmore, G., Wyse, R. F. G., & Kuijken, K. 1989, ARA&A, 27, 555
Hartwick, F. D. A. 1976, ApJ, 209, 418
Ibata, R. A., & Gilmore, G., 1995. MNRAS, 275, 605
Jones, J. B., Gilmore, G., & Wyse, R. F. G. 1995a, MNRAS (in press)
Jones, J. B., Wyse, R. F. G., & Gilmore, G., 1995b, PASP, 107, 632
Kuijken, K., & Gilmore, G. 1989, MNRAS, 239, 605
Lacey, C. G. 1991, in Dynamics of Disc Galaxies, edited by B. Sundelius (Göteborgs University, Göteborg), p. 257
Laird, J., Rupen, M. P., Carney, B., & Latham, D. 1988, AJ, 96, 1908
Magain, P. 1987, A&A, 179, 176
Majewski, S. R. 1993, ARA&A, 31, 575
Marquez, A., & Schuster, W. J. 1994, A&AS, 108, 341
McWilliam, A. 1990, ApJS, 74, 1075
Nissen, P. E., Gustaffson, B., Edvardsson, B., & Gilmore, G. 1994, A&A, 285, 440
Norris, J., & Ryan, S. 1989, ApJ, 340, 739
Norris, J., & Ryan, S. 1991, ApJ, 380, 403
Ojha, D. K., Bienayme, O., Robin, A. C., & Mohan, V. 1994, A&A, 290, 771
Olsen, E. H. 1983, A&AS, 54, 55
Pagel, B. E. J. 1989, in Evolutionary Phenomena in Galaxies, edited by J. E. Beckman and B. E. J. Pagel (CUP, Cambridge), p. 201
Pagel, B. E. J., & Patchett, B. E. 1975, MNRAS, 172, 13
Quinn, P. J., Hernquist, L., Fullagher, D. P. 1993, ApJ, 403, 74
Ryan, S. G., & Norris, J. E. 1993, in Galaxy Evolution: The Milky Way Perspective, edited by S. R. Majewski (ASP, San Francisco), p. 103
Sandage, A. 1969, ApJ, 158, 1115
Saxner, M., & Hammarbäck, G. 1985, A&A, 151, 372
Schmidt, M. 1963, ApJ, 137, 758
Schuster, W. J., & Nissen, P. E. 1989a, A&A, 221, 65
Schuster, W. J., & Nissen, P. E. 1989b, A&A, 222, 69
Sommer-Larsen, J. 1991, MNRAS, 249, 368
Sommer-Larsen, J., & Antonuccio-Delugo, V. 1993, MNRAS, 262, 350
Tinsley, B. 1975, ApJ, 197, 159
Tosi, M. 1988, A&A, 197, 33
Truran, J. W., & Cameron, A. G. W. 1971, Ap. Sp. Sci., 14, 179
VandenBerg, D. A. 1985, ApJS, 58, 711
VandenBerg, D. A., & Bell, R. A. 1985, ApJS, 58, 561
VandenBerg, D. A., & Laskarides, P. G. 1987, ApJS, 64, 103
Bergh, S. van den 1962, AJ, 67, 486
Wyse, R. F. G. 1995, in Stellar Populations, IAU Symposium No. 164, edited by P. C. van der Kruit and G. Gilmore (Kluwer, Dordrecht), p. 133
Wyse, R. F. G., & Gilmore, G. 1992, AJ, 104, 144
Wyse, R. F. G., & Gilmore, G. 1994, in Physics of the Gaseous and Stellar Disks of the Galaxy, edited by I. R. King (ASP, San Francisco), p. 201